FINAL TECHNICAL REPORT

NEW AGE CONSTRAINTS FOR THE TIMING OF PALEOEARTHQUAKES ON THE WESTERN GARLOCK FAULT

Implications for Earthquake Recurrence, Fault Segment Interaction, and Regional Patterns of Seismicity in Southern California

U.S. Geological Survey National Earthquake Hazards Reduction Program
External Grant Award Numbers 04HQGR0106 (ECI) and 04HQGR0084 (USC)

Recipients
Earth Consultants International
1642 E. 4th Street, Santa Ana, CA 92701
Phone: (714) 544-5321; Fax: (714) 494-4930
Web: www.earthconsultants.com
and
Department of Earth Sciences
University of Southern California
Los Angeles, CA 90089-0740
Phone: 213-740-8599; Fax 213-740-8801
Web: http://www.usc.edu/dept/earth/

Principal Investigators
Christopher Madden and James Dolan
madden@earthconsultants.com and dolan@usc.edu

Program Element III
Research on earthquake occurrence, physics and effects

Key Words
Paleoseismology, Quaternary Fault Behavior, Earthquake Recurrence, Segment Interaction, Fault Interaction

October 2008

Research supported by the U.S. Geological Survey (USGS), Department of the Interior, under USGS award number (Recipient, insert award number). The views and conclusions contained in this document are those of the authors and should not be interpreted as necessarily representing the official policies, either expressed or implied, of the U.S. Government.

ABSTRACT

New paleoseismic investigations on the western segment of the Garlock fault at Twin Lakes, California, reveal evidence for four well-defined surface ruptures and two other possible events during the past ~5,600 years. Although two of the well-defined earthquakes were previously identified at the site (Stepp et al., 1980), their timing was not well constrained. Calibrated radiocarbon dates from AMS analysis of detrital charcoal collected during our investigation constrain the timing of the four well-defined events at Twin Lakes to post-**A.D. 1450 (event A), 40 B.C. - A.D. 650 (event E)**, **770-360 B.C. (event G),** and **3620-2040 B.C. (event I).** Our investigation provides the first precise age constraints for events on the western segment of the Garlock fault and thus offers new insights into mid- to late Holocene behavior of the western and central segments of the fault. The timing of the most recent event (A) on the western segment is likely correlative with the most recent event (W) identified on the central segment at El Paso Peaks (A.D. 1450-1640; Dawson et al., 2004) and other sites, suggesting that the two segments rupture together during at least some very large ruptures. Interestingly, between 1 ka and 2 ka the central Garlock fault generated a cluster of three surface ruptures (Dawson et al., 2003; their events U, R, and Q), whereas the western Garlock fault at Twin Lakes experienced only one well-determined event (E). These observations suggest that in at least some instances the western Garlock fault breaks independently from the central part of the fault. An even more pronounced example of this behavior is Twin Lakes Event G, which occurred between 770 and 360 B.C., during a long lull in surface ruptures on the central Garlock fault. These results reveal a complicated pattern of strain release on the Garlock fault in which the western and central parts of the Garlock fault rupture together in some large-magnitude earthquakes, but sometimes rupture independently of one another, presumably in smaller-magnitude events. Rupture from one segment to another may be impeded by a 2-km-wide, extensional step-over between the segments at Koehn Lake. The addition of the western Garlock fault Twin Lakes data, particularly the occurrence of Event G during a pronounced lull in seismic strain release at 2-5 ka in the Mojave section of the eastern California shear zone (ECSZ), calls into question previous suggestions that the Garlock fault usually ruptures in phase with the ECSZ faults. In contrast, these new data appear to support the suggestion that seismic strain release on the Garlock fault may be more in phase with energy release on the Mojave section of the SAF and the Transverse Ranges faults of the Los Angeles region.

Awards 04HQGR0106
04HQGR0084

INTRODUCTION

The sinistral Garlock fault extends for 250 km from its intersection with the San Andreas fault near Frazier park in the west to its intersection with the southern end of the Death Valley fault system in the Avawatz mountains in the east (Figure 1). The fault is broadly arcuate in plan view and separates the Tehachapi-Sierra Nevada and Basin and Range provinces on the north from the Mojave block on the south. McGill and Sieh (1991) divided the fault into three segments based on significant bends or steps along the fault: a prominent 3.5-km wide left step at Koehn Lake separates the western segment from the central segment, and a 15° bend south of the Quail Mountains marks the boundary between the central and eastern segments.

The Garlock fault has not generated a large surface-rupturing earthquake in historical time. To help forecast future large earthquakes and potentially reduce earthquake losses, we must rely on paleoseismic records to understand the spatial and temporal pattern of fault behavior.

This study refines and extends the record of paleoearthquakes on the western Garlock fault. Recently, a long (8000 yrs) and detailed paleoseismic record was recovered from the central Garlock fault (Dawson et al., 2003). The new paleoseismic data we present here for the western Garlock fault allow us to compare the timing of events on the western and central segments, as well as to evaluate the Garlock's relationship to the San Andreas (SAF), Eastern California Shear Zone (ECSZ), and Los Angeles-region fault systems. Specifically, our results allow us to address the following models, fundamental concepts and questions:

(1) How does the western segment of the Garlock fault interact with the central segment? Do both the western and central segments of the fault typically rupture together in system-wide ruptures, or do they rupture separately in smaller-magnitude earthquakes. Given the potential of a fault as large as the Garlock to generate large-magnitude (Mw>7.5) earthquakes, these results have obvious seismic hazard implications both for the southern California region as a whole, and especially for several rapidly urbanizing cities that lie in close proximity to the fault (e.g., Bakersfield, Lancaster, and Palmdale).

(2) How does the Garlock fault interact with other faults in southern California? Rockwell et al. (2000) showed that we are currently in a period of accelerated seismic moment release in the Mojave section of the Eastern California Shear Zone (ECSZ), with an ongoing cluster of earthquakes during the past ~1,000 years. Dawson et al. (2003) suggested that earthquakes on the central segment of the Garlock fault are generally "in phase" with active periods along the ECSZ. Does the western Garlock reveal a similar relationship to the ECSZ seismic clusters? Or do different

parts of the Garlock interact differently with the various major fault systems in this part of southern California? In contrast to the Dawson et al. (2003) suggestion that the central Garlock fault ruptures in phase with the ECSZ faults, Dolan et al. (2007) suggested that the Garlock, together with the Mojave-Big Bend section of the SAF and Transverse Ranges faults in the Los Angeles region, forms a mechanically integrated fault system that "trades off" activity with the ECSZ. In this model, Garlock fault seismic strain release is largely out of phase with periods of heightened activity on the faults of the Mojave section of the eastern California shear zone (ECSZ).Do earthquakes on the western Garlock better correlate with clusters and lulls on the ECSZ, as suggested by Dawson et al. (2003), or with the SAF+Transverse Ranges fault network, as suggested by Dolan et al. (2007)? If this latter view is correct, we might expect to see Garlock fault earthquakes occurring in close temporal association with earthquakes in the Los Angeles region and with periods of heightened activity along the Mojave section of the SAF and the faults of the Los Angeles region.

Previous Paleoseismic Studies Along the Garlock Fault

The majority of investigations along the Garlock fault over the past several decades have aimed at determining slip rates. For example, Laviolette et al. (1980) estimated a 1.6-3.3 mm/yr slip rate based on 300 m sinistral offset of channels, which are incised into a Pleistocene surface in Oak Creek Canyon (Figure 1). A 5-8 mm/yr rate was determined by measuring the offset of a late Pleistocene gravel bar at Koehn Lake (Clark and Lajoie, 1974, Clark et al., 1984). A similar, and better-documented 90 m offset of a Searles Lake shoreline dated at 11,200 ^{14}C years B.P. yields a preferred slip rate of 5-7 mm/yr (McGill and Sieh, 1993). Troxel et al. (1972) suggested that the slip rate of the Garlock from the central to the western segment. New results, however, from geomorphic analysis of a ≥66 +/- 6m offset channel at Clark Wash near Lone Tree Canyon appear to contradict this view (McGill et al., 2003; in press).Specfically,radiocarbon dating of detrital charcoal and measurements of the offset channel at Clark Wash indicate a calibrated slip rate at least 7.6 +3.1/- 2.3 mm/yr for this site along the western Garlock fault. These results indicate a consistent slip rate across the Koehn Lake stepover between the central and western Galrock fault segments (McGill et al., in press). Excavation across another channel at this site shows the occurrence of at least two-three earthquakes in the past 2550 +/- 200 cal years B.P, yielding an average recurrence interval less than 1500 years (Figure 2). The slip rate of the Garlock fault appears to be faster than the geodetically constrained rate of elastic strain ccumulation. In fact, several geodetic studies suggest that there may be essentially zero strain accumulation along the western Garlock (e.g., Savage and ?, 10990; Peltzer et al., 2001). In contrast, a recent study (McClusky et al., 2001) using GPS strain rates as a constraint on a block model estimated 4.0 +/- 0.7 mm/yr slip rate for the western segment Garlock. Even this faster block-model rate is lower than the geologic rate, however, suggesting that strain accumulation and release rates along the Garlock fault are not constant in time.

With the notable exception of the McGill and Rockwell (1998) and Dawson et al. (2003) studies of the El Paso Mountains site (discussed below), there have only been a few dedicated paleoseismic studies along the Garlock fault, and most of these have yielded limited constraints on the timing of paleoearthquakes. In an excavation in Searles Valley (Figure 2), however, charcoal ages from a faulted layer indicate the most recent earthquake in this area occurred after A.D. 1460 (McGill, 1994b). This earthquake must have occurred before A.D. 1900 based on the lack of historical large earthquakes along the Garlock fault (Figure 2).

To date, the most comprehensive paleoseismic study on the western segment of the Garlock fault was located in the Tehachapi Mountains at Twin Lakes (Stepp et al., 1980). There, a shutter ridge forms a closed basin in which a sag pond has developed. An excavation across the pond revealed evidence for multiple earthquakes in about the last 3,000 years (kyr). Stepp et al., (1980) interpreted two events, with the penultimate rupturing before 2800 +/- 165 ^{14}C years B.P. and the most recent event (MRE) after 890 +/- 195 ^{14}C years B.P. From these data they estimated approximate recurrence intervals on the order of 1000+ years (Laviolette, et al., 1980). We note that the detailed study titled *Seismic Hazard of the Western Portion of the Garlock Fault* was published as Stepp et al. (1980). However, the shorter summary of these results by Laviolette, et al. (1980) is more commonly cited.

While this previous work has provided valuable input to calculate average recurrence intervals along the Garlock fault (Table 1), these studies have not been able to precisely constrain the ages of individual faulting events, primarily due to either limited amounts of datable material or undeveloped dating techniques. For example, the original Twin Lakes study by Stepp et al.(1980) was conducted prior to the advent Accelerator Mass Spectrometry (AMS).

Thus, these previous studies have not been able to address the question of whether the recurrence interval is regular, clustered, or irregular, nor have they been able to ascertain the timing of events on the Garlock fault relative to events on the Eastern California Shear Zone (ECSZ), the San Andreas fault, or the faults of the Transverse Ranges in the Los Angeles area.

Table 1. Summary of Recurrence Interval Estimates for the Garlock Fault

Fault Section	Site Location	Average Recurrence Interval (years)	Reference
Western	Campo Teresa	800-1600	ECI unpublished report
Western	Twin Lakes	> 1900	inferred from *LaViolette et al.* [1980]
Western	Lone Tree Canyon	700-2700	*McGill* [1994 a, b]
Western	Lone Tree Canyon	<1500	*McGill* [2003]
Central	Koehn Lake	900-1700	*Burke* [1979] and *Burke and Clark* [1978]
Central	El Paso Peaks	700-1200	this study
Central	Christmas Canyon	< 1670	inferred from *Roquemore et al.* [1982]
Central	Pilot Knob Valley	200-1300	*McGill and Sieh* [1991]
Eastern	Leach Lake and Avawatz Mountains	200-3000	*McGill and Sieh* [1991]

Modified from McGill and Rockwell, (1998) Table 3

In contrast to the western segment of the Garlock fault, a trench site on the central segment, located 2.3 km west of U.S. Highway 395 in the El Paso Peaks, has revealed a detailed history of Garlock fault earthquakes since eight thousand years ago (8 ka) (McGill and Rockwell, 1998; Dawson et al., 2003). The El Paso Peaks trench site, which was located where a shutter ridge ponded fine-grained alluvium, exhibited exceptionally continuous, thin-bedded stratigraphy and abundant detrital charcoal, allowing these researchers to identify six paleo-surface ruptures (Table 2).

Table 2. Ages of Faulting Events at the El Paso Peaks site from Dawson et al., (2003)

Event	Preferred Age	From Interpolated Sedimentation Rate
W	A.D. 1540	A.D. 1450-1640
U	A.D. 810	A.D. 675-950
R	A.D. 375	A.D. 250-475
Q	A.D. 160	A.D. 25-275
K	3140 B.C.	3340-2930 B.C.
F	4840 B.C.	5000-4670 B.C.

The event ages shown in Table 2 reveal an irregular pattern of recurrence, with the most recent four events rupturing in the past 2 kyr, preceded by an approximately 3,000-year-longquiet period. This clustered behavior on the central

Garlock does not fit traditional log normal recurrence models. A similarly long earthquake record from the western segment is required for comparison with the central segment. Such a record, which forms the focus of this study, would allow for comparison with central Garlock fault results and facilitate evaluation of the Garlock fault's relationship to other southern California fault systems.

Over the past decade numerous researchers have generated sufficient paleoseismic data from most of the major (e.g., SAF, ECSZ, LA region) to begin to understand and model long distance and long term fault interaction. For example, Dawson et al., (2003) suggested that, in general, the central Garlock earthquakes appeared to correlate with seismic clusters on faults of the ECSZ in the Mojave desert (Rockwell, et al., 2000). Dolan et al., (2007) note similar clustered behavior along faults in the greater Los Angeles metropolitan area. Their analysis, however, indicates that Los Angeles-area are anti-correlated with ECSZ events over the past 11 ka. Moreover, they suggest that the Garlock fault actually slips largely in concert with periods of heightened activity on the SAF and faults of the Los Angeles-region as part of a mechanically integrated fault system, rather than together with the ECSZ faults. In this context, the absence of data from the western segment represents one the most significant gaps in our ability to accurately model these regional fault interactions.

Motivation for Revisiting Twin Lakes

A literature review, aerial photo analysis and field reconnaissance to identify trench sites on the western Garlock fault showed Twin Lakes to be the most promising site for constraining paleo-earthquake timing. One of the primary reasons is that the site is one of the few places between Bear Trap and Oak Creek Canyons where the fault trace hasn't been obscured by landsliding, and can be easily identified (Clark, 1973). Furthermore, Stepp et al. (1980) showed that the Twin Lakes site preserves a record of paleoearthquakes, although age constraints from their study were poor. Finally, our review of trench logs from Stepp et al. (1980) suggested to us that evidence for additional surface ruptures may have been exposed in their trenches, leading us to revisit the site.

Hand-auger samples that we collected from the site contained detrital charcoal that could be dated using AMS radiocarbon dating, a methodology that wasn't available at the time of the investigation by Stepp et al. (1980). Thus, stratigraphy and events at the site could be dated at much higher resolution than was possible with the bulk-soil samples used in the earlier study. Lastly, Twin Lakes is relatively far from the SAF (40 km), suggesting that it may not be strongly affected by potential complications associated with triggered slip induced by SAF earthquakes.

Awards 04HQGR0106
04HQGR0084

RESULTS

Site Geomorphology

At the Twin Lakes site, left-lateral slip on the Garlock fault has generated a one-kilometer-long, west-northwest trending shutter ridge, which partially ponds a small basin (1.3 km^2) draining the south flank of Liebre Twins Mountain in the Tehachapi Range (Figure 1 and 3). The "lake" at Twin Lakes is a seasonal sag pond that has formed in the resulting valley. The lake receives sediment from three primary sources: (1) Fluvial and debris flow deposits from a deeply incised canyon in the flank of the mountain northwest of site; (2) Colluvium and landslide debris from the steep slopes to the north and south of the lake; and (3) Alluvial fans that empty from rills cut into steep hillslopes to the north and south. Debris from a landslide on the north side of the lake is being re-deposited in the center of the lake as an alluvial fan.

Aerial photo mapping by Clark (1973), together with surface mapping in this study, revealed a series of degraded and discontinuous scarps that were most likely formed during the most recent surface-rupturing earthquake (Figure 3). The westernmost distinctive scarps are located ~500 m west of the lake. However, based on Stepp et al.'s (1980) western trench (hereafter called trench S1), fault strands pass near the central and southern end of the current lake (Figure 3). To the east, fairly continuous scarps extend to within 200 m of the lake and project into the south side of an anomalously high, elongate ridge on the south side of the lake (Figure 3). Based on this mapping, we conclude that Stepp et al. (1980) did not find the fault in their second trench (S2) because the fault steps to the right to join the fault projection on the east side of the lake somewhere between their two trenches – this was later confirmed in our trenches TW1 and TW2 Figures 3 and 4). Clark (1973) mapped the fault here as a subtle right bend that continues through the length of the lake. This geometry cannot be correct given the lack of faulting in Stepp et al.'s (1980) trench S2. This right step occurs in the vicinity of the topographic high, which is most likely a pressure ridge linking the surface breaks. Based on our trenching results, the main strand of the Garlock fault follows the southern margin of the lake, with discontinuous secondary strands extending into the center of the lake.

Paleoseismic Excavations

We excavated two approximately north-south trenches across the Garlock fault at the Twin Lakes: Trench TW1 (45 m long by 4- to 4.5-m-deep) was excavated across a significant fault splay near the center of the lake (Figures 3 and 4). We located the trench approximately 3 m west of the Stepp et al.'s trench S1 to help facilitate the correlation of stratigraphic units and faults between the trenches. The goals of this trench were to collect datable organic material to bracket the timing of paleo-earthquakes identified in S1 and to look for evidence of additional ruptures possibly missed by Stepp et al., (1980).

We placed trench TW2 (35 m long by 1.5- to 2-m-deep) approximately 100 m east of TW1, about half way between Stepp at al.'s trenches S1 and S2. Trench TW2 was placed to intersect the westward projection of the primary fault strand from TW1, to an area where it is being buried by the distal margin of a fan sourced from the shutter ridge to the south. The goal of this trench was to recover a better stratigraphic record of events along the main strand, which was almost completely obscured by bioturbation in trench TW1. As in trench TW1, however, stratigraphic relations in TW2 were also heavily bioturbated and difficult to interpret along the main fault strand.

We excavated a third trench, TW3 across a small closed depression southeast of the main lake and along the projection of a subtle scarp in an alluvial fan to the west of the depression. This trench did not reveal any evidence of faulting and is not described further in this report. Including cutting back the walls of the fault zone in TW1, our study provided six new exposures of the Garlock fault zone at Twin Lakes. Below we describe our findings from the best exposures from our Twin Lakes trenches, focusing mainly on observations from both walls of TW1 and a one-m cut into the east wall of TW1.

Stratigraphy and Faulting

The Twin Lakes sag pond is filled with thinly to coarsely bedded, sandy and clayey silts interbedded with thin packages of fluvial sand and a bed of matrix-supported gravel (Figure 5). The fluvial sand units typically have sharp lower contacts, whereas sandy silts and clays have gradational lower contacts, suggesting that the sag has two primary modes of deposition: cut and fill, and settling out of suspension. The sequence of fine grained units at the site coarsens upwards from clayey silt to sandy silt. Many of the finer-grained units are also locally capped by buried soil A horizons, indicating that the deposition rate in the sag ponds is often slow enough to allow for significant soil development. The sand layers are well sorted, suggesting that they were deposited by single flood events. Depositional contacts are disturbed by bioturbation throughout the trench, making them locally irregular, especially close to the ground surface.

Sag-pond deposits pinch out toward the northern and southern margins of the lake. Near the southern shoreline of the lake, most sag deposits pinch out near the northern edge of a diffuse, 7-m-wide zone of faulting (Strand 2 on Figure 4). Stratigraphy in the fault zone consists of massive, highly bioturbated colluvium, locally interbedded with thin, discontinuous sag deposits. The southern end of the fault zone is bounded by a significant fault that juxtaposes colluvium on the north against oxidized and calcified older alluvium on the south (Strand 3 on Figure 4). The juxtaposition of such disparate units across this strand 3 is indicative of significant offset, suggesting that this strand marks the main trace of the Garlock fault.

In trenches TW1 and S1, some beds pinch out northward toward a secondary zone of faulting in the center of the lake (Figure 6; Strand 1 on Figure 4). This fault is defined by a single strand near the base of the trench, which splays upward. Units can be traced across this fault zone and have an apparent vertical separation that is up to the north. Figure 5 shows a stratigraphic column for a topographic low on the downthrown side of the fault 1 in trenches TW1 and S1 (Figure 6). With each earthquake, accommodation space for deposition is created in this portion of the lake bed, thus preserving the most complete record of deposition in the trench exposures.

The stratigraphy in the upper ~1.5 m of the column contains massive, sandy silts (Units 10, 20, 30, 35, 50, 70, and 90) interbedded with distinctive, thin, pale- and dark-brown silt and clay beds (25, 40, 60, 80, 95). Between 1.5 and 2.7 m below the ground surface, dark-brown, organic-rich clayey silts (120, 150) are interbedded with pale-brown, upward-coarsening couplets of clayey to silty sand overlain by a bed of coarser sand (100+110, 130+140, 160). We interpret the dark brown organic units to be paleosols. Between 1.7 and 3.6 m depth, a bed of sandy silt with fine gravel (170) overlies a distinctive clast-supported gravel (180), which in turn overlies three pale-brown sand beds (190, 200, 210). We interpret the gravel as a reworked landslide, likely sourced from the steep slopes to the north. The overlying sandy silt with gravel is likely a debris flow. The sand beds below the gravel coarsen upward, with the basal sand containing significant clay, and the upper sand bed consisting of coarse sand. Between meters 3.6 and 4.25 depth is a dark-brown, fine-grained sandy silt (220), locally with fine-grained sand interbeds (230).

The stratigraphic section north of the fault is incomplete due to erosion and non-deposition on the upthrown block. Although most units are correlative across the fault zone, some units, such as 100, 170, 200, and 210 thin markedly northward. Units 110, 130+140, 160, 165, and locally 190 pinch out northward on the south side of the fault zone.

Geochronology

We collected more than 40 samples of detrital charcoal from trench TW1. Of these, 10 samples were sent for AMS ^{14}C dating at Lawrence Livermore National Laboratory. Samples for dating were selected to bracket paleo-earthquakes, and to provide age control for as many units as possible. Most of the coarser-grained units (110, 130, 140, 170, 180, 190, and 200) did not contain detrital charcoal.

Radiocarbon ages were calibrated and statistically analyzed using Oxcal 3.1 (Bronk Ramsey, 2004; usingatmospheric data from Reimer et al., 2005). Figure 6 shows the stratigraphic location and ages of the samples selected for dating. Ages are reported in calibrated calendric dates. Because ages are derived from detrital charcoal, these dates must be considered maximum ages due to the potential for long residence time of detrital charcoal before deposition at the Twin Lakes site.
Six of the 10 samples were in correct stratigraphic order. However, most samples that were out of stratigraphic orderyielded ages that were statistically similar to samples from adjacent, or nearby beds. For example, dates from silt beds 40 and 60 contain radiocarbon dates of 1515 +/-40 years and 1345 +/- 40 years, respectively, but when taking into account the stratigraphic ordering of each

sample to trim age probability curves in the calibration program, these samples yielded nearly identical ages of A.D. 580 - 655 and A.D. 565 – 650, respectively. Samples in units 210 and 220 returned radiocarbon ages that were nearly identical, with the age from unit 210 only 5 years older tha-n the sample below (4705 +/-35 vs. 4700 +/- 35). After incorporating stratigraphic constraints and calibration, however, the ages were identical at 3620-3360 BC. These radiocarbon dates reveal that the stratigraphic section exposed in TW1on the south side of the fault extends from the mid-Holocene to the present. The stratigraphic and geochronological resolution is too coarse, however, to reliably resolve variations in deposition rate for different units.

Evidence for Paleo-earthquakes

Several types of stratigraphic and structural relations define paleoearthquake event horizons at the Twin Lakes site. In general, we do not consider the presence of single indicator as strong evidence for an event. Rather, we believe the presence of several different event indicators at the same stratigraphic level in the same trench, and across several different trench faces, is strong evidence for a paleoearthquake horizon.

For example, pinching of stratigraphic units towards the fault zone is strong evidence for an earthquake horizon, especially when the thinning occurs at the same stratigraphic level as a step in vertical separation of faulted units. This suggests that there is a recurrent vertical component of slip at Twin Lakes that produces scarps against which lake deposits pinch out.

Unconformities marked by the upward termination of fault strands against unbroken capping beds are considered good event evidence only if the unconformity is found on multiple walls. We consider a single upward termination to be poor evidence for an event.

Finally, differential warping or folding of units adjacent to the fault zone is considered strong evidence for a faulting event when corroborated by other lines of evidence.

Faulting Events

Stratigraphy in trench TW1 records evidence for four well-defined surface ruptures, as well as for two other possible events. Events are designated from youngest to oldest, A, E, G, and I; the two possible events are designated as C and K. Each alternate letter is skipped to reserve them for the possibility that the stratigraphic record is incomplete, and not all events have been recorded at the site. Figures 6 – 8 show the fault zone in the west and east walls of trench TW1, and a one-m cut into the upper half of the east wall, respectively. On each log, event evidence is labeled with the event designator and a subscript denoting the type of evidence. Subscripts include *p* for pinching of units against a paleoscarp, *t* for upward termination of a fault strand against an unbroken overlying unit, and *w*, for differential warping between different units. We employ this same nomenclature to previously published of the logs of the west and east walls of trench S1, which we have re-interpreted for this study based on the findings from adjacent trench exposures (Figures 9 and 10). Table 3 summarizes evidence related to each event found in the trench wall exposures. In the following section, we describe in detail the evidence for each of the four well-defined paleo-surface ruptures that we identify at Twin Lakes.

Table 3. Correlative paleoearthquake evidence in Twin Lakes trench exposures

		Trench Wall Exposures				
		TW1 W Figure 6	**TW1 E** Figure 7	**TW1 cut, E** Figure 8	**S1 W** Figure 9	**S1 E** Figure 10
Event Evidence	A	T 10 P 10	T 10	T 10	T 10+	T 10+
	E	No clear evidence	T 70 or 80, W 80	T 80-	No clear evidence	No clear evidence
	G	P 110, W 100?	P 110 T 110 -	P 100-110	P 110	T 100-, P? 100
	I	P 130-165 T 165-	P 130-160 T 160 -	N/A	P 130-165; T 170 W? 170	No evidence

T 10 - fault strand is truncated by an unconformity at the base of unit 10. Minus sign after number indicates that fault strands cannot be traced confidently to the base of the terminating unit. A + sign indicates the fault dies out within the united numbered.
P 10 – unit 10 pinches out towards fault zone
W 80 – unit 8 is warped upward more than units above

Event A

The most recent well-defined surface rupture (A) at the Twin Lakes site is expressed in all exposures of TW1 and S1 by upward terminations of major fault strands within the modern soil (unit 10), (Figures 6 – 10). Trench logs by Stepp et al. (1980) show fault strands cutting the base, but not the top, of unit 10, suggesting that the ground surface was lower at the time of the event, although it is possible that the shallowest evidence for the event A has been obscured by post-event soil-forming processes. The west wall of TW1 clearly shows thinning of unit 10 northward across the fault zone, suggesting that the upper part of this unit is filling against a paleoscarp produced by surface rupture from event A (Figure 6).

The highest potential stratigraphic level for event horizon A is the base of unit 10. However, the horizon could occur as low as the contact between units 10 and 25.

Vertical separation of units 40 through 80 between event A and the penultimate event horizon varies between 59 and 89 cm in the TW1 and S1 exposures. In TW1, vertical separations are 10 to 20 cm higher on the west wall than the east wall, and in trench S1 vertical separations of these units are up to 21 cm higher on the east wall than on the west wall. These variations suggest that a significant component of the offset measured for beds that can be correlated across the fault is produced by the juxtaposition of dipping beds or irregular topography by lateral movement of the fault.

On the flat surface of the sag pond, the pinching of units against paleoscarps is a much better measure of the true vertical component of deformation. This measurement is only a minimum due to possible erosion of the fault scarp. Assuming that only one event occurs above unit 30, the thinning and pinching of units 10 through 25 across the fault zone in all exposures suggests a minimum of 45 cm of true vertical offset across the fault. Based on the thinning of the base of unit 10 across the fault, the absolute minimum vertical offset for event A is less than 10 cm. Taken together, the amount of apparent vertical slip and the true vertical slip for each event are a good proxy for the size of the events relative to one another.

Event E

Evidence for the penultimate surface rupture (Event E) is found only on the east wall and the cut of the east wall of trench TW1 (Figures 7 and 8). The east wall of the main trench revealed two fault splays that extend upward into the base of unit 90, but which cannot be traced further upward. A minor discontinuity in unit 80 in line with the projection of the faults may mark the upward continuation of these faults. However, unit 80 has many similar breaks that are not associated with faulting and that are likely due to bioturbation. North of the break, unit 80 is warped slightly upward, which could be due to upward continuation of the faults, or to drag on a primary fault strand to the north. Unit 60 is not deformed above the discontinuity.

In the cut of the east wall of TW1, a single fault strand extends upward into unit 90, where, as in the east wall, the fault is difficult to trace upward (Figure 8). The truncation of a fine-grained sand bed in line with the upward projection of the fault, approximately 15 cm below the top of unit 90 suggests the fault extends at least to this stratigraphic level. Unit 80 is clearly not broken in the cut wall exposure. Thus, we attribute the discontinuity in the east wall TW1 to bioturbation, and place event horizon E between the truncated sand at the top of unit 90 and the base of unit 80.

We found no evidence for event E in either wall of S1. Distributed, *enechelon* faulting during this earthquake may explain the lack of evidence in some trench exposures.

Based on the pinching of unit 90 towards the fault zone, the vertical component of deformation for event E was approximately 10 cm. The lack of significant changes in the thickness of units across the fault zone suggests that the horizontal component of slip for this event was small compared to event A.

Event G

The third event back (Event G) is expressed by the northward pinch-out of unit 110 toward the fault zone in all faces of TW1, as well as by the upward termination of a fault strand within 20 cm of the base of unit 110 in the east wall of

TW1 (Figure 6). We interpret the event horizon to be the contact of units 110 and 120. In exposures TW1 W and TW1 E, Unit 110 gradually pinches against unit 120, ~40 to 70 cm south of the fault zone (Figures 6 and 7). In the cut of the east wall of TW1, this unit pinches out abruptly at the fault zone. Approximately 2 m to the south, unit 110 pinches out in the west wall of trench S1, approximately two m south of the fault. The irregularity of the northern margin for unit 110 may be the result of warping of the ground surface by the mole track created during event G.

In contrast to unit 110, unit 100 does not pinch out completely, but thins across the fault zone. A minimum value for the vertical component of slip for event G is reflected in the maximum thickness of unit 110: ~15 cm. As with event E, we infer that the small vertical component of slip reflects rupture during a small earthquake, or perhaps the end of a larger rupture.

Event I

The pinching out of multiple units (130-165), measuring 40- to 60-cm-thick, against unit 170, suggests that event I probably had relatively larger displacement compared to other events identified in our trenches. All deep exposures at the site also revealed a fault strand extending into unit 170 and dying out upward without cutting the base of overlying units 150-160.

The thickness of units 130-165 provides a minimum constraint of 60- 70 cm for the vertical component of motion related to this event, which suggests this event was much larger than events E or G. Below the event horizon, the abrupt thickening of unit 160 across the fault from the downthrown block to the up-thrown block suggests significant lateral slip during event I.

Based on deformation related to each event, we believe that events A and I were large compared to events E and G.

Other event indicators

We reserve K for a possible earlier event in our exposures. The primary evidence for a potential event K is the pinching of unit 190 toward the fault zone and an upward termination of a single fault strand below unit I in the east wall of trench TW1. Because unit 190 may appear on both sides of the fault in the east wall of TW1 and in the east wall of TW2, we are not sure if the pinching reflects an irregular channel margin, or pinching against a broad, irregular warp caused by event K. The upward fault terminantion below unit 190 is by itself not convincing, either. More work will need to be done to determine whether the contact between units 180 and 190 is really an event horizon.

Timing of Paleoearthquakes at Twin Lakes

We constrain the timing of events at the Twin Lakes site with bracketing AMS ^{14}C ages from detrital charcoal samples. Table 4 compares the timing of events from our study to previous constraints on event timing at Twin Lakes (Stepp et al., 1980). To facilitate this comparison, we have calibrated the bulk-soil ages of Stepp et al. (1980) using the same methodology as for our detrital charcoal ages.

A detrital charcoal sample from the top of unit 20, the shallowest faulted unit in the Twin Lakes excavations, yielded a calibrated radiocarbon age of A.D. 1450-1650. Thus, the most recent event on the Garlock fault at Twin Lakes occurred post-1450. We do not think that the sample has been bioturbated into the deposit because it was collected from consolidated, unbioturbated sediment. The minimum age is not constrained by geochronologic data. It is unlikely that any large magnitude (M>7) earthquakes on the western Garlock would have remained unrecorded in the historic record after ~ 1850. Thus, our best estimate of the MRE at the Twin Lakes site is between 1450 and 1850.

Detrital charcoal samples from units 60 and the base of unit 90 bracket the timing of event E between 40 B.C. A.D. 350. A sample from the stratigraphic level of the event horizon near the top of unit 90 yielded an age of A.D. 80 – 250, and may date the event horizon.

Event horizon G is stratigraphically constrained by units 110 and 120, and locally by 100 and 120. Detrital charcoal samples from the base of unit 100 and the top of unit 120 closely bracket the timing of event G between 770 and 360 B.C.

Detrital charcoal samples from units 150 and 210 provide poor constraints on the timing of event I, which occurred between the deposition of units 150 and 170. Thus, we are only able to say that Event I occurred between 3620 and 2040 B.C.

Table 4. Revised Timing of Faulting Events at the Twin Lakes Site

This study		Stepp, et. al. 1980)
Event	Age	Age
A	1450 – 1800 A.D.	Post A.D. 711-1415
E	40 B.C. – 650 A.D.	Not identified
G	770-360 B.C.	Not identified
I	3620-2040 B.C.	Pre 1426-544 B.C.

DISCUSSION

The Twin Lakes site reveals evidence for at least four well-defined surface ruptures-on the western part of the Garlock fault during mid- to late Holocene time. Although the temporal distribution of events on the western Garlock suggests slightly more regular recurrence of earthquakes than on the central Garlock fault.

The age constraints provided by our study are not good enough to fully test this assumption.

Comparison between El Paso Peaks/Twin Lakes results

Comparison of the new event record from Twin Lakes with palaeoseismological results from the central Garlock fault allows us to begin to discern patterns of rupture during mid-to late Holocene time (Figure 12). At their El Paso Peaks site, Dawson et al. (2003) saw evidence for six earthquakes in the past 7500 years; five of these events occurred during the time period exposed at Twin Lakes. The MRE (Event A) at the Twin Lakes site occurred after 1450 and before ~1850. These age constraints are similar for the MRE at El Paso Peaks (post 1450 to 1650). Thus, the MRE at both site could be the same earthquake. This inference is bolstered by two independent observations: (1) McGill and Sieh (1993) and Dawson et al. (2003) note that the smallest offsets of geomorphic features near El Paso Peak are about 7 m, suggesting that the MRE on the central Garlock was a very large-magnitude (Mw => 7.5), consistent with rupture of the entire Garlock fault; and (2) Vertical separation across the mid-basin strand at Twin Lakes of 65 to 75 cm was the largest of any of the four well-constrained events that we measured, consistent with the possibility of large horizontal displacements at the Twin Lakes site during this earthquake.

Dawson et al. (2003) observed a cluster of three events between 0 and 1000 AD. Within this same interval, we see evidence for only one well-determined event (Event E). Event E generated a relatively small, >25cm tall scarp across the basin flat, suggesting that this event had a relatively small horizontal displacement at Twin Lakes.

Two alternative interpretations of these data are that: (1) one of the three events measured by Dawson et al. (2003) also ruptured the Western Garlock as Event E; or (2) all of the three central Garlock earthquakes were restricted to that part of the fault, and Event E represents a western-Garlock-only rupture.

Event G at the Twin Lakes site occurred during an interval with no recorded earthquake on the central Garlock fault, suggesting that this event was limited to the western part of the fault. This is consistent with the observation that event G had a significantly smaller vertical component of slip than event A. Conversely, Event I had the largest measured vertical component of slip of the four events recorded in TW1, suggesting a large-magnitude, and therefore possibly system-wide, rupture.

Dawson et al. (2003) suggested, on the basis of their El Paso Peaks trench results, that the Garlock fault ruptures in concert with the faults of the Mojave section of the ECSZ (Figure 12). A compilation of paleo-earthquake ages from the Mojave region by Rockwell et al. (2000) reveals three robust features: (1) an ongoing cluster of large-magnitude earthquakes during the past ~1,000 years, but possibly extending slightly further back in time to ~ 2ka; (2) a pronounced lull in seismic activity between at least 2 ka and ~5ka; and (3) a second cluster of earthquakes between 5 ka and 6 ka. Dawson et al. (2003) note that they observe an apparently large-displacement surface rupture between 145-1650 AD, which clearly occurred during the ongoing ECSZ cluster. They also note the occurrence of a cluster of three central-Garlock fault surface ruptures between 0 and 1,000 AD, which they suggest also occurred during the ECSZ cluster. We note, however, that the most pronounced part of the current ECSZ cluster occurred during the past ~1,000 years, and that the possible heightened period of seismic moment release shown on figure 12 between 0 and 1,000 AD is at least partially a function of the fact that the ages of several of the youngest earthquakes compiled by Rockwell et al. (2000) are not well constrained. Specifically, some of them are constrained by only maximum-possible ages. Thus, the probability distribution functions for moment release through time for these events are potentially skewed towards the oldest-possible part of the ongoing cluster, and the period of apparently slightly heightened ECSZ moment release between 0 and 1,000 AD may be at least partially an artifact of imprecise dating of these ECSZ earthquakes.

In contrast, as noted by Dolan et al. (2007), the three 0-1,000 AD, central-Garlock surface ruptures documented by Dawson et al. (2003) fall well within the time range of the well-constrained cluster of large-magnitude earthquakes that occurred at ~ 1,000-2,500 years ago on the faults in the Los Angeles region (Figure 12). Similarly, Weldon et al (2004) have suggested on the basis of data from their Wrightwood site that the Mojave section of the SAF has been slipping somewhat slower (~23 mm/yr) than its long-term average slip rate (≥~31 mm/yr) during the past ~1100 years. This period of relatively slow SAF slip followed a period of apparently exceptionally fast slip on the SAF that overlaps with at least the latter part of the 1 ka-2.5 ka cluster of Los Angeles-region earthquakes. In addition to these data, geodetic observations suggest apparently slower-than-average rates of elastic strain accumulation along the SAF and Garlock faults, and faster-than-normal rates of strain accumulation along the ECSZ faults (e.g., Savage et al., 1990; Peltzer et al., 2001; Oskin et al., 2008). These relationships prompted Dolan et al. (2007) to suggest a model in which the Pacific-North America plate boundary in southern California comprises two mechanically complementary fault systems. One system comprsise the Garlock fault, the Mojave and Big Bend sections of the SAF, and the faults of the Los Angeles region. The faults of the ECSZ and its extension to the north, the Walker Lane belt, together with the southern SAF system (which is common to both systems) comprise a second major fault system. These authors suggest that the two major faults wax and wane in opposition to one another, with the ECSZ system currently stroing and releasing energy faster than its long-term average rate. In contrast, Dolan et al. (2007) suggested that the SAF+Garlock+Los Angeles-region fault network is storing and releasing energy more slowly than its long-term average rate. They suggest that the roles of the two faults system was reversed starting ~1,000 years ago, with the ECSZ system moving into "slow" mode between ~1,000 and 5,000 years ago. This hypothesis is consistent with: (1) the occurrence of only one surface rupture on the Garlock during the past ~1,000 years, in contrast to the central Garlock cluster between 1 ka and 2ka; (2) the occurrence of the 1-2 ka central Garlock cluster of events during what Dolan et al. (2007) suggest was a period of heightened activity of the SAF+Garlock+LA-region system; and (3) the occurrence of our Twin Lakes Event G during the middle of the well-defined lull in ECSZ activity between 5 ka and 2 ka (and possibly <2ka, because as noted above, some of the ECSZ Mojave earthquakes are constrained only by maximum ages).

The Twin Lakes data thus add to a growing pool of paleo-earthquake data that is helping to constrain the behavior of the complicated network of faults that make up the Pacific-North America plate boundary in southern California. Although these new data provide the opportunity to directly compare the behavior of the central and western segments of the Garlock faults, one of the largest and fastest-slipping faults in the plate boundary, the age constraints on some of these events must be more tightly constrained to make further progress. Moreover, the possible occurrence of other events along the western Garlock that escaped our notice during the Twin Lakes study, either because they ruptured only the poorly defined main strand of the fault at Twin Lakes, or because they occurred on geomorphically subtle strands that we did not identify, needs to be clarified with future study. Finally, in order to fully understand the seismic behavior of the Garlock, detailed paleoseismologic data are needed from the eastern part of the fault.

CONCLUSIONS

New paleoseismic results from the western Garlock fault constrain the timing of four well-defined events at Twin Lakes to post-A.D. 1450 (event A), 40 B.C. - A.D. 650 (event E), 770-360 B.C. (event G), and 3620-2040 B.C. (event I). Although some of these events overlap with the timing of events at the El Paso peaks site of Dawson et al. (2003) along the central part of the fault, and may possibly record the same large-magnitude, system-wide ruptures, the timing of other paleo-earthquakes differs between the two sites. These observations suggest that the Garlock fault sometimes ruptures in its entirety, but at other times ruptures are sresticted to eother the central or western parts of the fault, possibly in response to rupture arrest at the extensional step in the fault at Koehn Lake. The timing of paleo-earthquakes at the two sites, particularly at the western Twin Lakes site, does not match well the timing of seismic clusters in the eastern California shear zone. Rather, we follow Dolan et al. (2007) in suggesting that the Garlock fault paleo-earthquake ages appear to be better explained by the Garlock fault moving mainly in concert with the Mojave section of the San Andreas fault and with the faults of the Los Angeles region, possibly in response to periods of faster-than-normal elastic strain accumulation caused by long-distance and long-term fault interactions amongst the major fault systems of the Pacific-North America plate boundary in southern California.

REFERENCES

Clark, M. M., 1973, Map showing recently active breaks along the Garlock and associated faults, Californian: U.S. Geological Survey Map I-741.

Dawson, T. E., McGill, S. F., and Rockwell, T. K., 2003 in press, Irregular recurrence of paleoearthquakes along the central Garlock, near El Paso Peaks, California: Journal of Geophysical Research.

Dolan, J. F., Bowman, D. D., and Sammis, C. G., 2007, Long-distance and long-term fault interactions in southern California: Geology, v. 35, p. 855-858.

Fumal, T. E., Pezzopane, S. K, Weldon, R. J. II, and Schwartz, D. P. , 1993, A 100-year average recurrence interval for the San Andreas fault at Wrightwood, California, Science, v. 259, p. 199-203.

Fumal, T. E., Weldon, R. J., II, Biasi, G. P., Dawson, T. E., Seitz, G. G., Frost, W. T., and Schwartz, D. P., 2002, Evidence for large earthquakes on the San Andreas fault at the Wrightwood, California, paleoseismic site: A.D. 500 to present, Bulletin of the Seismological Society of America, v. 92, p. 2726-2760.

Grant, L. B., and K. Sieh, 1994, Paleoseismic evidence of clustered earthquakes on the San Andreas fault in the Carrizo Plain, California, Journal of Geophysical Research, v. 99, no. B4, pp. 6819-6841.

Keller, R. P., Allen, C. R., Gilman, R., Goulty, N. R., and Hileman, J. A., 1978, Monitoring slip along major fault in southern California: unpub. Cal Tech report.

LaViolette, J. W., G. E. Christenson, and J. C. Stepp, Quaternary displacement on the western Garlock fault, southern California, in Fife, D. L. and A. R. Brown, eds., Geology and Mineral Wealth of the California Desert, Santa Ana, California, South Coast Geol. Soc., 449-456, 1980.

McClusky, S. C., S. C. Bjornstad, B. H. Hager, R. W. King, B. J. Meade, M. M. Miller, F. C. Monastero, and B. J. Souter, Present day kinematics of the Eastern California Shear Zone from a geodetically constrained block model, Geophys. Res. Lett., 17, 3369-3372, 2001. 2001.

McGill, S. F. and K. Sieh, 1991, Surficial offsets on the central and eastern Garlock fault associated with prehistoric earthquakes, Journal of Geophysical Research, v. 96, p. 21,597-21,621.

McGill, S. F., and Kerry Sieh, 1993, Holocene Slip Rate of the Central Garlock Fault in Southeastern Searles Valley, California: Journal of Geophysical Research v.98, p. 14,217-14,231.

McGill, S. F., 1994a, Preliminary slip rate and recurrence interval for the western Garlock fault near Lone Tree Canyon, California, Geological Society of America, Abstracts with Programs, v. 26, p. 72.

McGill, S. F., 1994b, Holocene activity on the central Garlock fault, in: Geological Investigations of an Active Margin, Geological Society of America, Cordilleran Section Guidebook, edited by Sally F. McGill and Timothy M. Ross, published by San Bernardino County Museum Association, pp. 356-364.

McGill, S. F. and Rockwell, T. K., 1998, Ages of late Holocene earthquakes on the central Garlock fault near El Paso Peaks, California: Journal of Geophysical Research, v.103, no.B4, p7265-7279.

McGill, S. F., et al., 2003, Slip rate of the western Garlock fault near Lone Tree Canyon, Mojave Desert, California, Geological Society of America, Abstracts with Programs.

McGill, S. F., Wells. S. G., Fortner, S. K., Kuzma, H. A., and McGill, J. D., in press, Slip rate of the western Garlock fault at Clark Wash, near Lone Tree Canyon, Mojave Desert, California: Geol. Soc. Amer. Bull., in press, 2008.

Rockwell, T. K., Lindvall, S., Herzberg, M., Murbach, D., Dawson, T., and Berger, G., 2000, Paleoseismology of the Johnson Valley, Kickapoo, and Homestead Valley Faults: Clustering of Earthquakes in the Eastern California Shear Zone: Bulletin of the Seismological Society of America, Vol. 90, No. 5, pp. 1200-1236.

Sieh, K. E., Stuiver, M., and Brillinger, D., 1989, A more precise chronology of earthquakes produced by the San Andreas fault in southern California: Journal of Geophysical Research, v. 94, p. 603-623.

Stepp, C. J., LaViolette, J. W., and Christenson, G. E., 1980, Seismic Hazard of the Western Portion of the Garlock fault, U.S. Geological Survey open file report No. 80-1172.

Stuiver, M., and Reimer, P. J., 1993, Extended 14C database and revised CALIB radiocarbon calibration program, Radiocarbon, 35:215-230.

Troxel, B. W., Wright, L. A., and Jahns, R. H., 1972, Evidence for differential displacement along the Garlock fault zone, Californian, Geological Society of America, Abstracts with Programs, v. 4, n. 3, p. 250.

Weldon, R. J., II, Fumal, T. E., Powers, T. J., Pezzopane, S. K., Scharer, K. M., and Hamilton, J. C., 2002, Structure and earthquake offsets on the San Andrea fault at the Wrightwood, California, paleoseismic site, Bulletin of the Seismological Society of America, v. 92, p. 2074-2725.

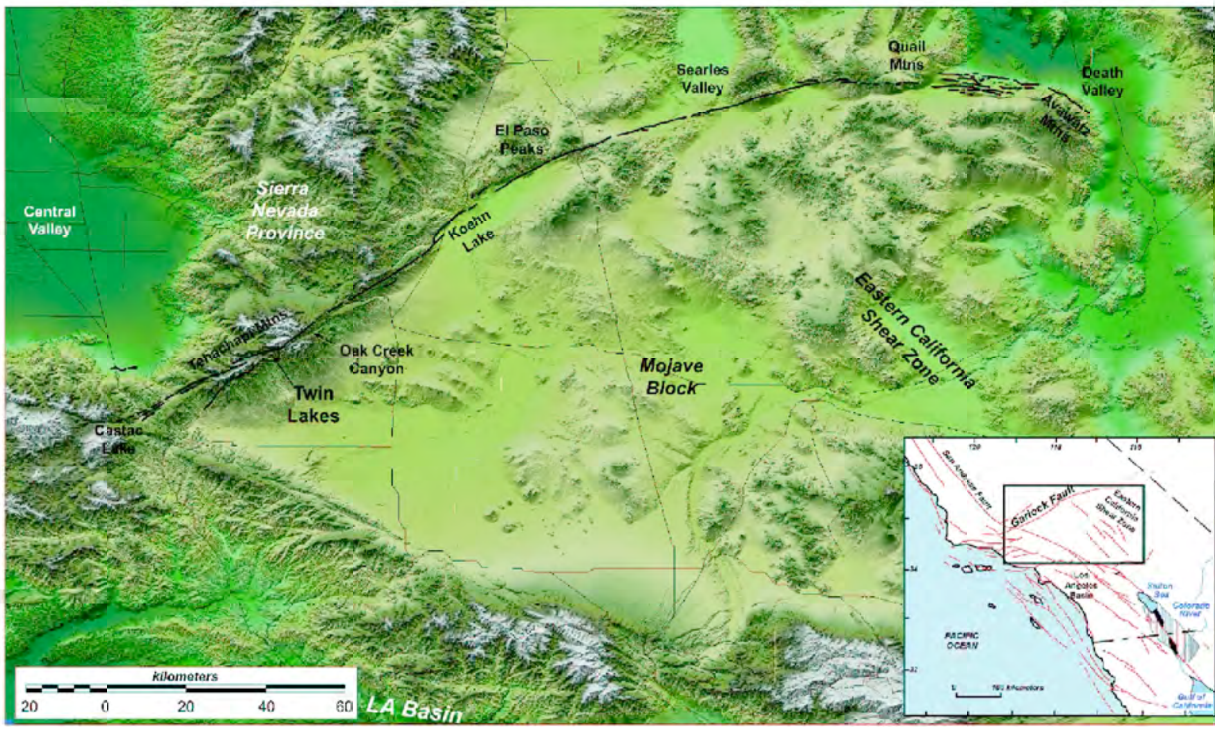

Figure 1. Regional location map showing the Garlock fault trace (thick black line; Jennings, 1994), major tectonic provinces, and key geographic locations along the Garlock fault. Thin black lines mark the major highways and small black box near Twin Lakes shows the location of Figure 3. Inset shows active faults in southern California and Mexico in red and the location of the main figure outlined by the black box.

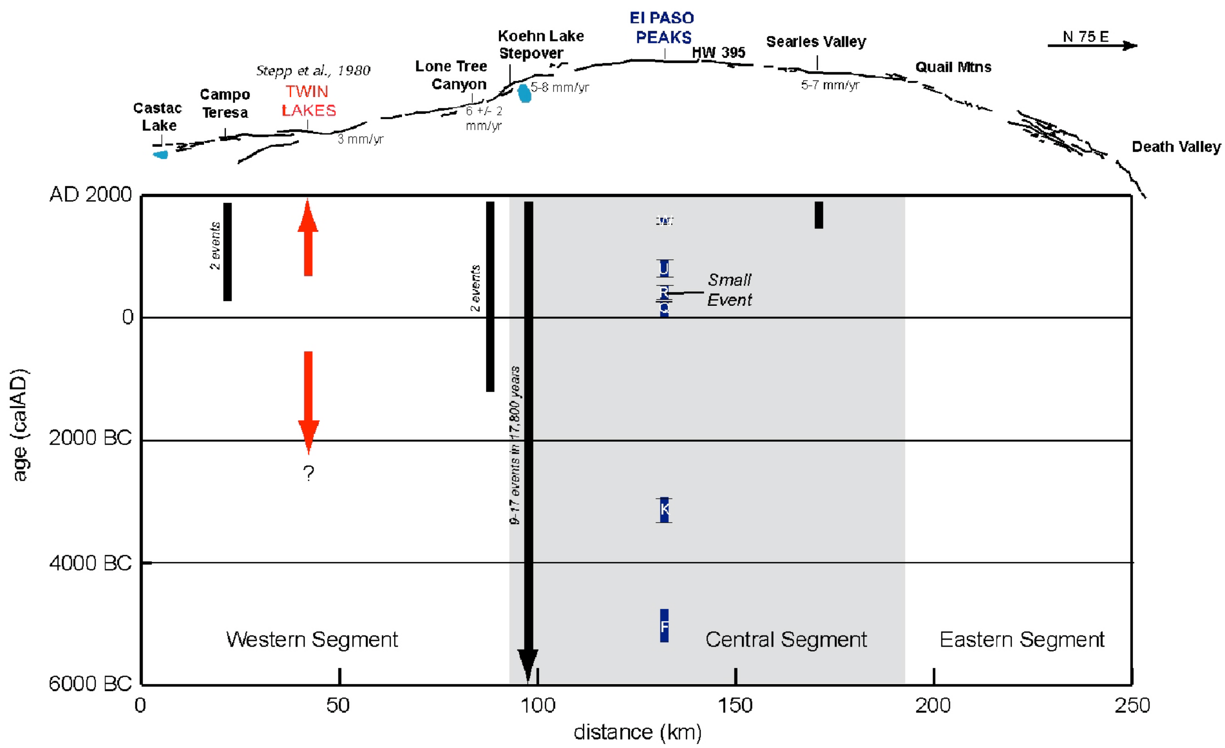

Figure 2. Event chronology and slip rate data versus distance along the Garlock fault. The vertical bars show the 2 sigma upper- and lower-most calender ages for the bracketing radiocarbon samples. Arrows indicate an open-ended constraint. Note the strip map at the top of the figure for reference (Jennings, 1994). The only previous well-dated paleoseismic site on the Garlock was located at El Paso Peaks (blue bars; Dawson et al., 2003; McGill and Rockwell, 1998). Prior to our study, paleoseismic work at Twin Lakes found evidence for only two earthquakes in the last >3000 years (red bars; Stepp et al., 1980). Although these results could be interpreted to suggest that the central segment ruptures far more frequently than the western segment of the fault, event ages at Twin Lakes were too poorly constrained to evaluate fault-segment interaction. Data from Searles Valley from McGill and Sieh (1993) and McGill (1994b). Lone Tree Canyon data from McGill (2003) and Koehn Lake slip rate from Clark et al. (1984). Original data reported in radiocarbon years B.P. was calibrated using Calib 4.3 (Stuiver and Reimer, 1993).

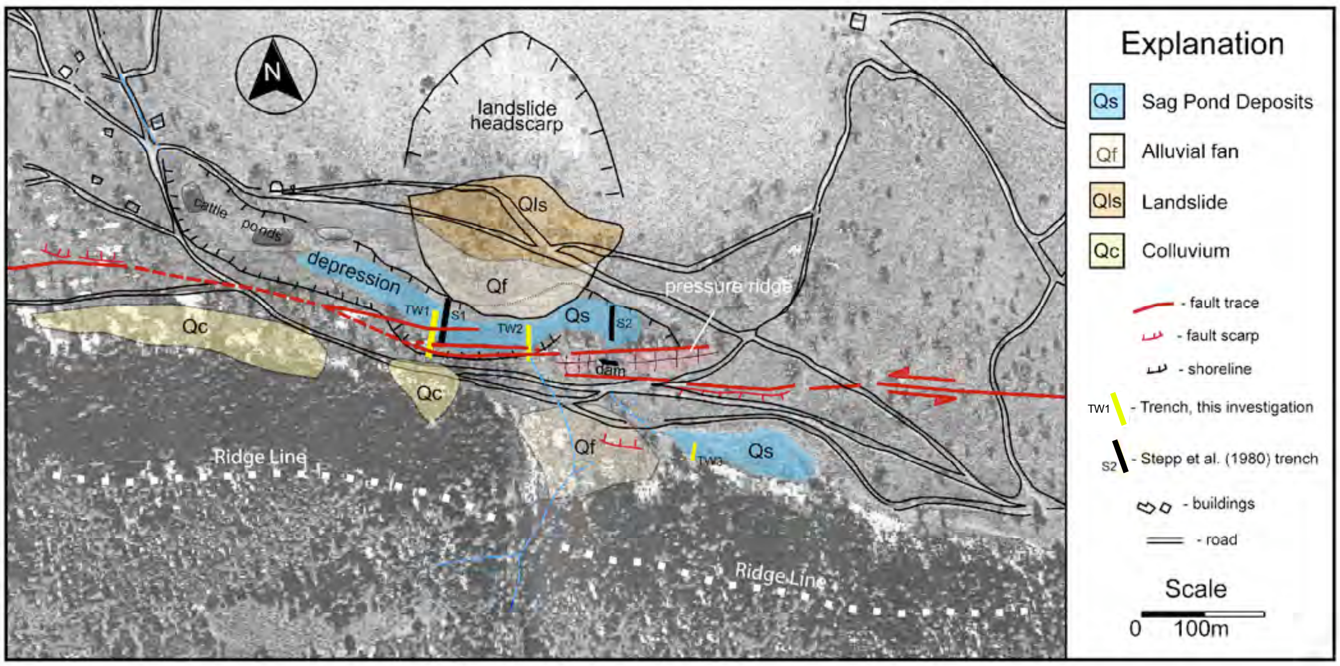

Figure 3. Map of the Twin Lakes site showing Quaternary deposits, the mapped trace of the Garlock fault, tectonic geomorphology, and trench sites.

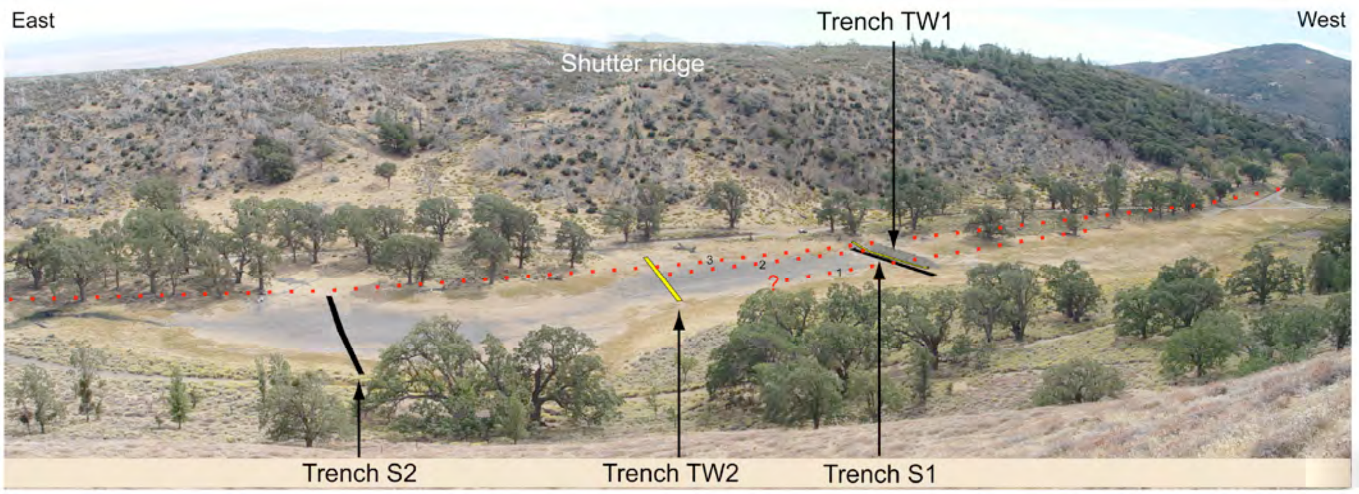

Figure 4. View to the south of Twin lakes in the foreground and a large shutter ridge in background. Strands of the Garlock fault that were identified in paleoseismic trenches are marked by dashed red lines. Stepp et al. (1980) exposed fault strand 1 near the center of the lake in their trench S-1. Trenches TW1 and TW2, excavated for our study, revealed that in addition to strand 1, other strands of the fault (2 and 3) run parallel to the southern margin of the lake.

Stratigraphy and Age of Twin Lakes Sag Pond Deposits

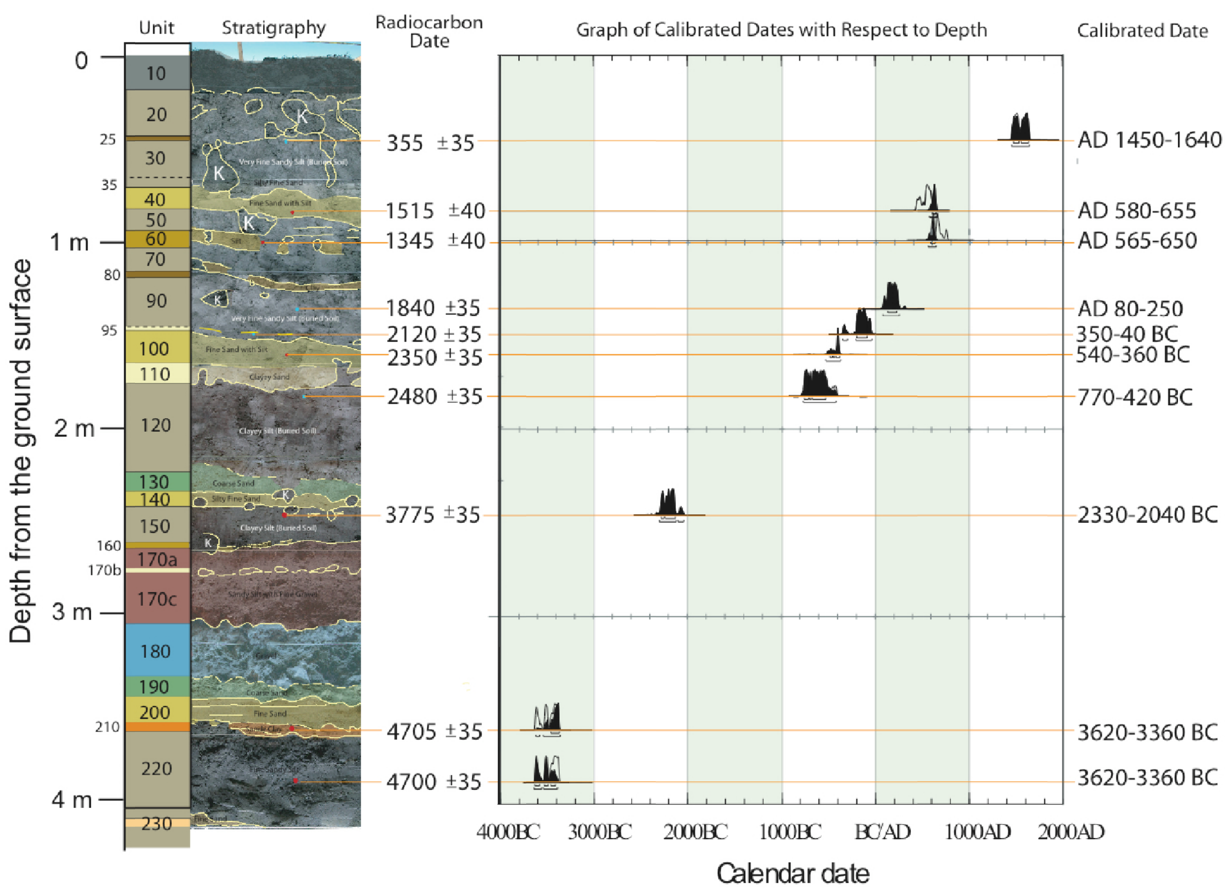

Figure 5. Composite stratigraphic section of units exposed in trenches TW1, TW2 (this study) and S1 (Stepp at al., 1980). The Twin Lakes sag pond is filled primarily with fine-grained deposits that have settled out of suspension (e.g., units 30, 90, and 120), interbedded with thin fluvial sands, silts (units 40 and 100 and 130), and in one case, a gravel-rich debris flow (unit 180). Ten charcoal samples returned radiocarbon ages that were mostly in correct stratigraphic order (left side of table). Radiocarbon ages were calibrated and statistically analyzed using Oxcal 3.1 (Bronk Ramsey, 2004) and atmospheric data from Reimer et al. (2005). Age probability distributions are clipped based on stratigraphic relations such that an age at a higher stratigraphic level cannot be older than an age from a lower stratigraphic level (right side of table).

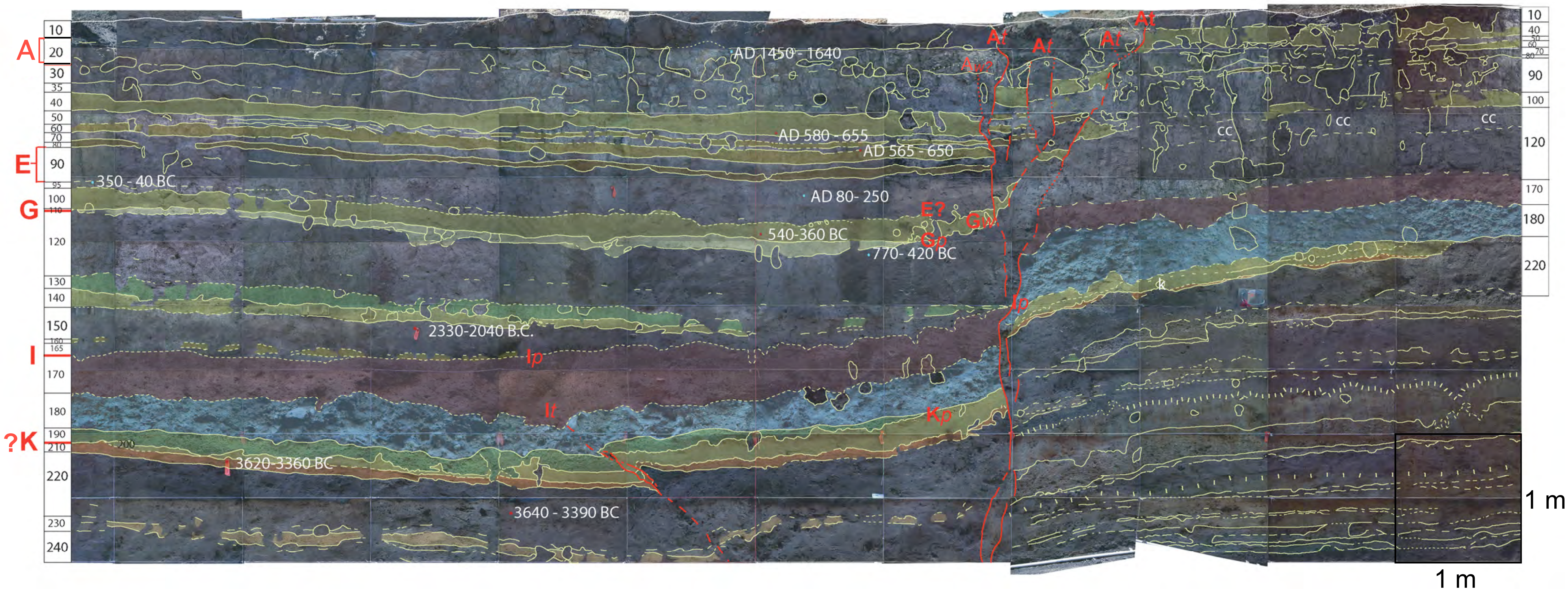

Figure 6. Photo-log of the west wall of trench TW1 across fault strand 1 (see Figure 4 for the location of the trench and fault strands). Stratigraphic units are colored to aid in correlation between different trench wall exposures. The fault is defined by a very narrow zone from the base of the trench to within ~2.5 meters of the ground surface, above which it splays upward into several strands. Event horizons A, E, G, I, and possible event horizon K is shown along the left side of the log. Evidence for each event is marked by the event designator, and letter symbol for the evidence: t for upward termination of a fault strand, p for pinching of a post event unit against an inferred paleoscarp, and w for differential warping of a unit with respect to overlying units. Locations and calibrated calendric ages of detrital charcoal samples shown in white. See Figure 5 and text for unit descriptions.

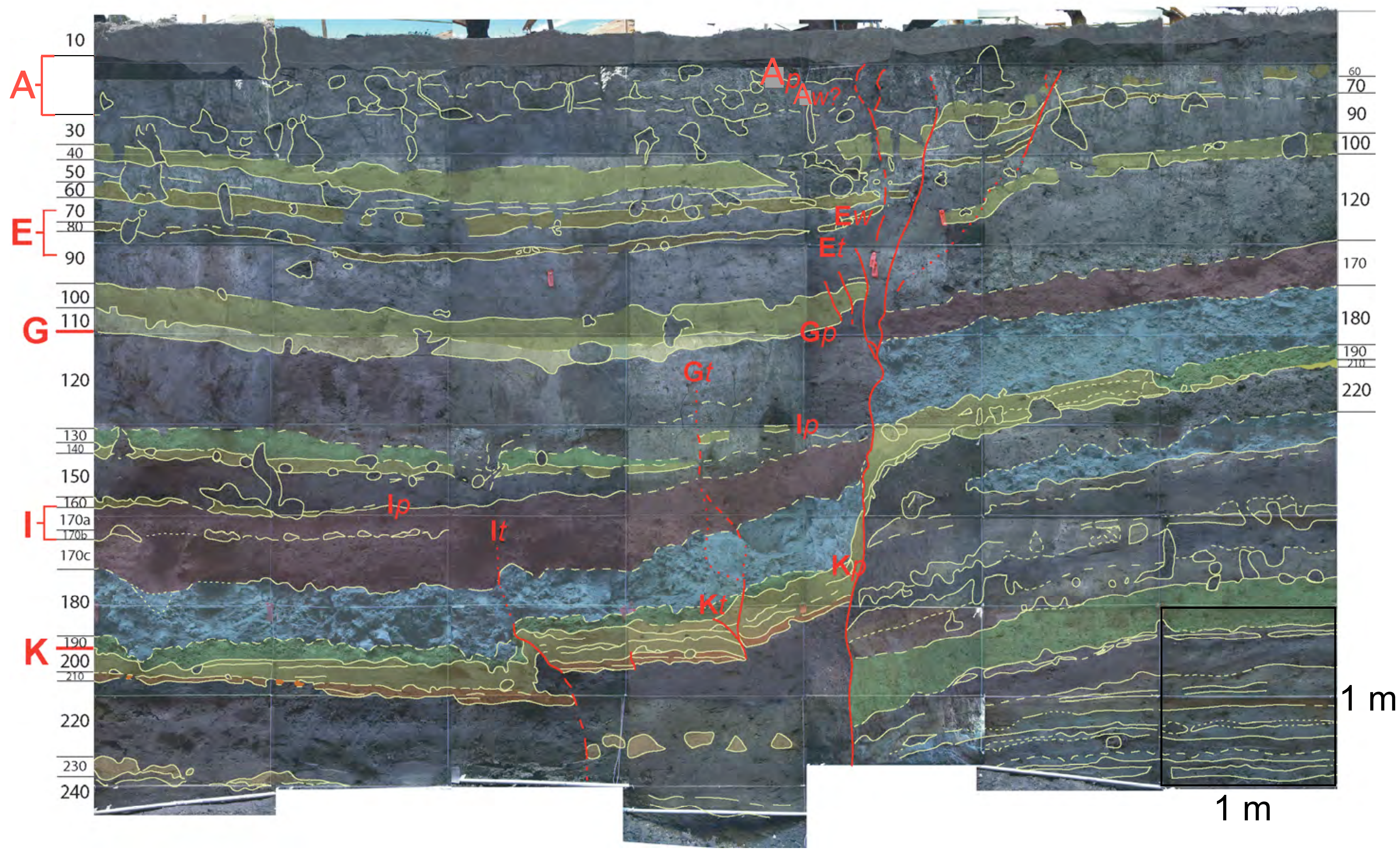

Figure 7. Photolog of fault zone 1 in the east wall of trench TW-1 (see Figure 4 for the location of the trench and fault strands). Event horizons A, E, G, I, and possible event horizon K are shown along the left side of the log. Evidence for each event is marked by the event designator, and letter symbol for the evidence: t for upward termination of a fault strand, p for pinching of a post event unit against an inferred paleoscarp, and w for differential warping of a unit with respect to overlying units.

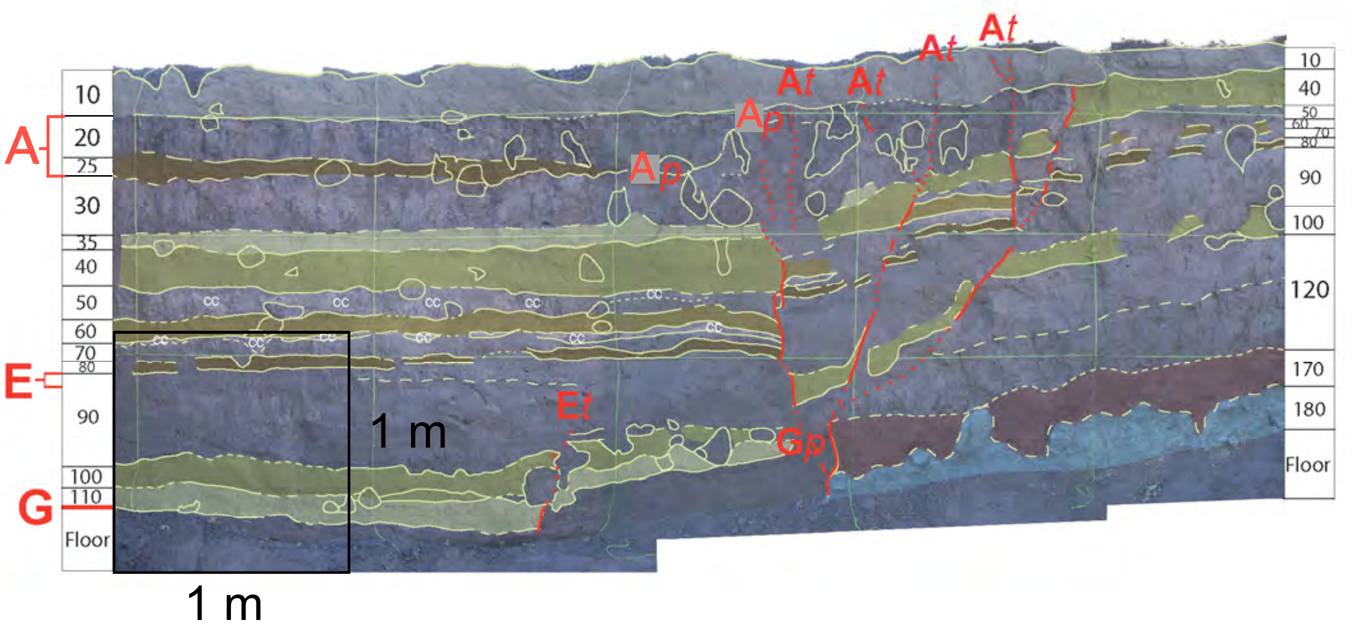

Figure 8. Photolog of a trench face cut ~1 m into the upper ~1.75 m of the east wall of trench TW-1. Event horizons A, E, G, are shown along the left side of the log. Evidence for each event is marked by the event designator, and letter symbol for the evidence: t for upward termination of a fault strand, p for pinching of a post event unit against an inferred paleoscarp, and w for differential warping of a unit with respect to overlying units.

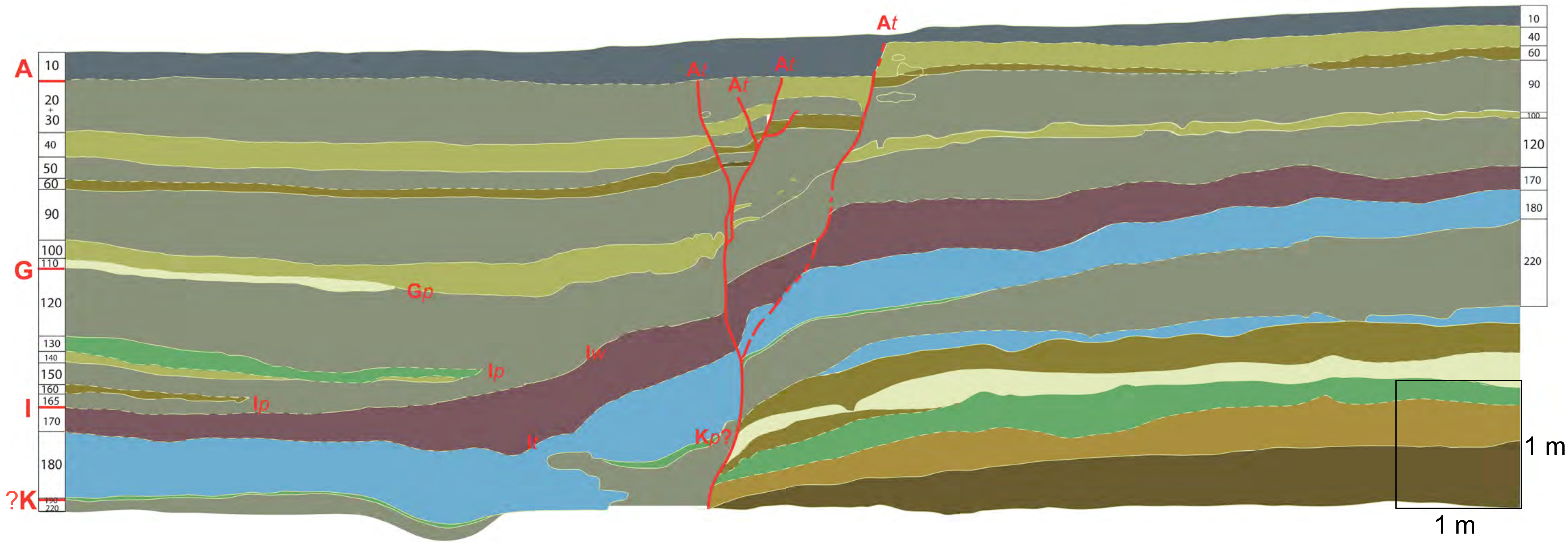

Figure 9. Log of the west wall of trench S1 from Stepp et al., 1980. Units have been renumbered to match the numbering scheme used for units identified trench TW-1. We have re-interpreted the location of event horizons and event evidence based on our findings in trench TW11. Event evidence includes: t for upward termination of a fault strand, p for pinching of a post event unit against an inferred paleo-scarp, and w for differential warping of a unit with respect to overlying units.

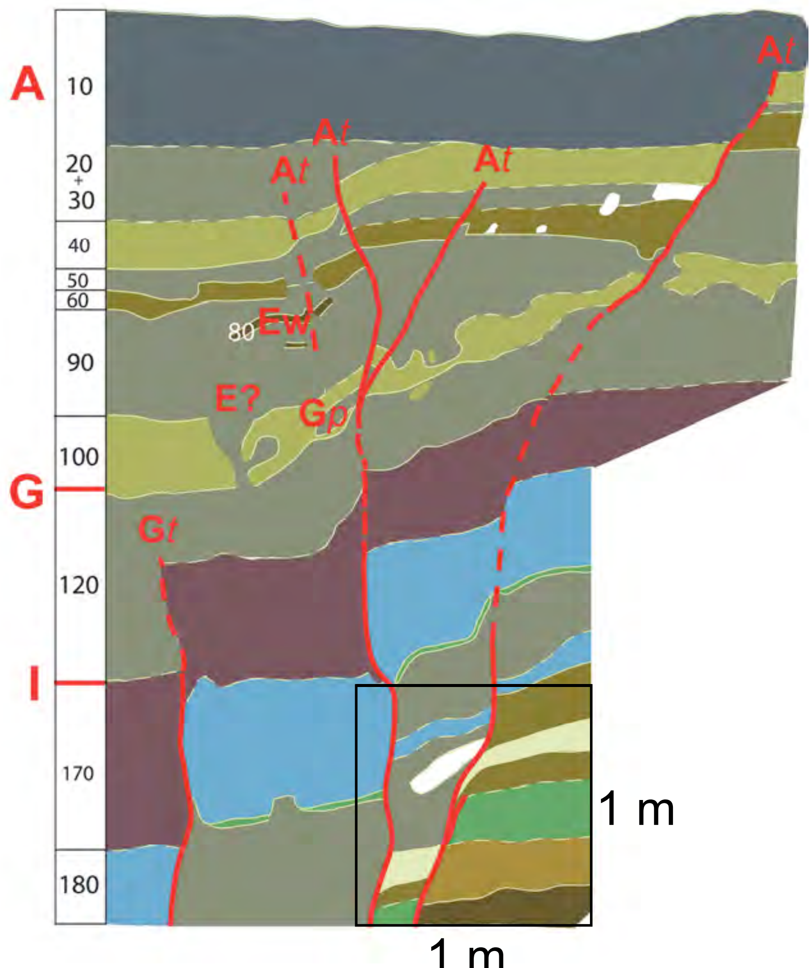

Figure 10. Log of fault zone 1 (see Figure 4) in the east wall of trench S1 from Stepp et al. (1980). Units have been re-numbered to match the numbering scheme used for units identified trench TW1. We have re-interpreted the location of event horizons and event evidence based on our findings in trench TW1.

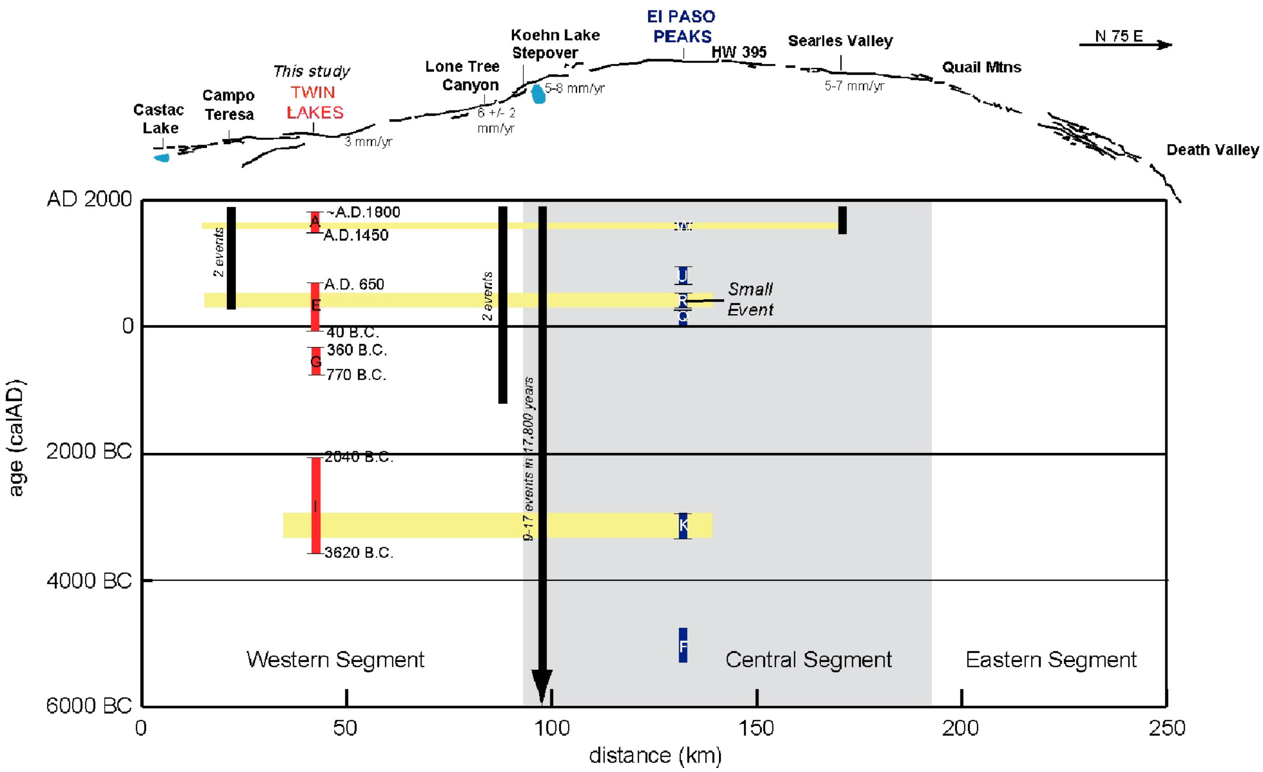

Figure 11. Comparison of new constraints on the timing of paleo-earthquakes at Twin Lakes (red bars), with existing paleoseismic data (black and blue bars) on the timing of paleo-earthquakes along the Garlock fault. Vertical bars show the 2 sigma upper and lowermost calender ages for the bracketing radiocarbon samples. Arrows indicate an open-ended constraint. Horizontal yellow bars mark permissible correlations of events between study sites along the Garlock fault. Although the resolution of the age constraints for ruptures is too poor to provide unequivocal correlations, large vertical separations for Twin Lakes (TL) event A (this study) and large horizontal offsets for El Paso Peaks (EP) event W (Dawson et al., 2003) suggest both sites probably ruptured during the same large-magnitude, system-wide earthquake. Similar evidence of large separations for TL event I, and EP event K suggest that these may also have been a single large-magnitude earthquake.

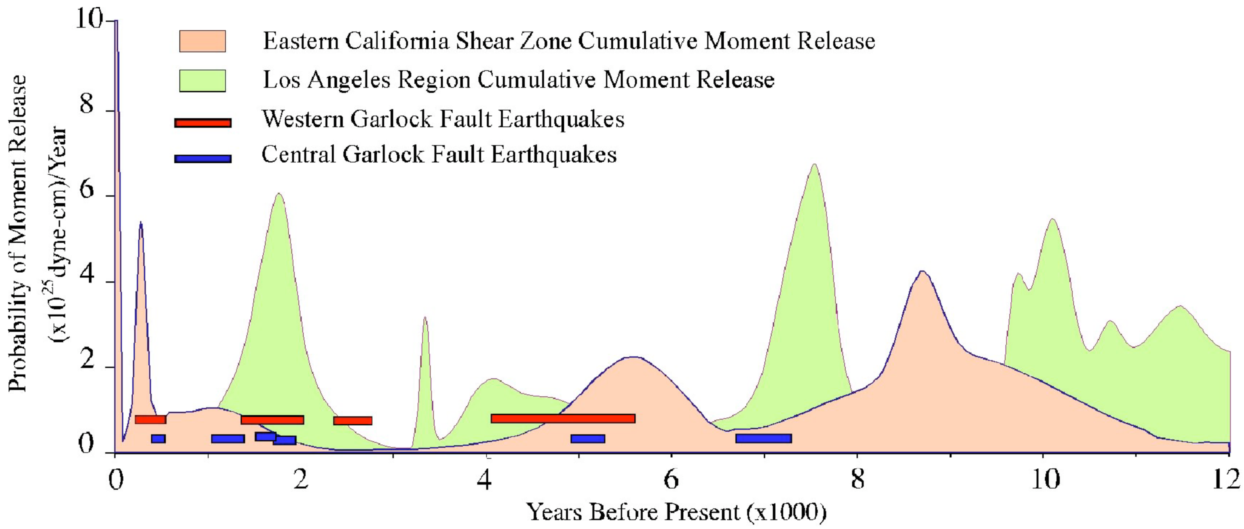

Figure 12. Comparison of patterns of strain release for faults in the Eastern California Shear Zone and the Los Angeles Basin with the western and central Garlock fault (modified from Dolan et al., 2007 with addition of paleo-earthquake data from Dawson et al., 2003 and this study).